Eur. J. Mineral.
2018, **30**, 581–592
Published online 20 December 2017

**Minerals and materials:
building principles and applications**

Lead-antimony sulfosalts from Tuscany (Italy). XXII. Marcobaldiite, $\sim Pb_{12}(Sb_3As_2Bi)_{\Sigma 6}S_{21}$, a new member of the jordanite homologous series from the Pollone mine, Valdicastello Carducci

Cristian BIAGIONI[1,*], Marco PASERO[1], Yves MOËLO[2], Federica ZACCARINI[3] and Werner H. PAAR[4]

[1] Dipartimento di Scienze della Terra, Università di Pisa, Via S. Maria 53, 56126 Pisa, Italy
*e-mail: cristian.biagioni@unipi.it
[2] Institut des Matériaux Jean Rouxel (IMN), Université de Nantes, CNRS, 2, rue de la Houssinière, BP 32229, 44322 Nantes Cedex 3, France
[3] Resource Mineralogy, University of Leoben, Peter Tunner Str. 5, 8700 Leoben, Austria
[4] Department of Chemistry and Physics of Materials, University, Jakob Haringerstr. 2a, 5020 Salzburg, Austria

Abstract: The new mineral species marcobaldiite, $\sim Pb_{12}(Sb_3As_2Bi)_{\Sigma 6}S_{21}$, has been discovered in a single specimen collected in a quartz vein embedded in tourmaline-bearing schist from the Pollone mine, Valdicastello Carducci, Pietrasanta, Apuan Alps, Tuscany, Italy. It occurs as a black blocky prismatic crystal, up to 1 cm in size, with a metallic luster, associated with Sb-rich tennantite. Under the ore microscope, marcobaldiite is white, with a distinct anisotropism, with grey to bluish-grey rotation tints. Polysynthetic lamellar twinning is common and characteristic. Reflectance percentages for the four COM wavelengths are [R_{min}, R_{max} (%), (λ)]: 31.6, 40.1 (470 nm), 30.9, 39.6 (546 nm), 30.4, 38.5 (589 nm), and 30.0, 37.6 (650 nm). Electron microprobe analyses gave (average of 10 spot analyses – in wt%): Pb 64.05(34), Bi 4.24(6), Sb 9.10(14), As 4.51(8), S 17.24(19), total 99.14(53). On the basis of $\Sigma Me = 18$ *apfu*, the empirical formula is $Pb_{11.98(4)}Sb_{2.90(3)}As_{2.33(3)}Bi_{0.79(1)}S_{20.80(20)}$. The main diffraction lines, corresponding to multiple *hkl* indices, are [*d* in Å (relative visual intensity)]: 3.568 (ms), 3.202 (ms), 3.016 (ms), 2.885 (ms), 2.233 (vs), 2.125 (s), 1.848 (s), and 1.775 (s). The crystal structure study gives a triclinic unit cell, space group $P\bar{1}$ with $a = 8.9248(9)$, $b = 29.414(3)$, $c = 8.5301(8)$ Å, $\alpha = 98.336(5)$, $\beta = 118.175(5)$, $\gamma = 90.856(5)°$, $V = 1944.1(3)$ Å^3, $Z = 2$. The crystal structure has been solved and refined to $R_1 = 0.067$ on the basis of 6188 reflections with $F_o > 4\sigma(F_o)$ and 363 refined parameters. Marcobaldiite is a new $N = 3.5$ homologue of the jordanite homologous series, characterized by the 1:1 alternation of two kinds of layers of distorted octahedra, three- and four-octahedra thick, *i.e.* of the kirkiite and jordanite types, respectively. Layers are connected by one atomic layer of three bicapped trigonal prismatic Pb atoms and one triangular pyramidal As atom in split position. The name of this new mineral species honours the mineral amateur Marco Baldi (b. 1944) for his contribution to the knowledge of the mineralogy of the pyrite ± baryte ± iron oxide ore deposits from southern Apuan Alps.

Key-words: marcobaldiite; new mineral; sulfosalt; crystal structure; lead; antimony; arsenic; bismuth; Pollone mine; Apuan Alps.

1. Introduction

The jordanite homologous series, first defined by Makovicky (1989), is a group of lead sulfosalts having general formula $Pb_{4N-2}Me^{3+}_6S_{4N+7}$, where Me^{3+} = As, Sb, Bi (Makovicky *et al.*, 2006). Three mineral species belonging to this series are reported in Moëlo *et al.* (2008), *i.e.* jordanite, geocronite, and kirkiite. The possibly related mineral tsugaruite, ideally $Pb_4As_2S_7$ (Shimizu *et al.*, 1998), has a different crystal structure (Matsushita *et al.*, 2014), even if its details have not been published yet.

Jordanite homologues are characterized by two short axes (~8.5 and ~9.0 Å) and a longer one, whose length depends on the homologue order, ranging from ≈26 Å ($N = 3$: kirkiite) to ≈ 32 Å ($N = 4$: jordanite and geocronite). The $N = 4$ isotypic pair jordanite ($Pb_{14}As_6S_{23}$) – geocronite ($Pb_{14}Sb_6S_{23}$) is well-known from various localities world-wide, and, considering also synthetic products (Jambor, 1969), displays a complete solid-solution. On the contrary, kirkiite, ideally $Pb_{10}As_3Bi_3S_{19}$, is exceedingly rare, having been described only in two localities, the Greek type locality (the Pb-Zn ore deposit of Aghios Philippos, near Kirki, Thrace; Moëlo *et al.*, 1985), and the high-T fumaroles of La Fossa crater, Vulcano, Aeolian Islands, Italy (Borodaev *et al.*, 1998; Pinto *et al.*, 2006).

In order to fully characterize the occurrence of geocronite from the Pollone mine, near the small hamlet of Valdicastello Carducci, Apuan Alps, Italy, where this mineral has been known since the first description given by Kerndt (1845), Biagioni *et al.* (2016a) examined both historical as well as new samples from this locality, studying them through single-crystal X-ray diffraction and electron-microprobe analysis. During this investigation, a

https://doi.org/10.1127/ejm/2018/0030-2710

0935-1221/18/0030-2710 $ 5.40

Table 1. Sulfosalts identified in the Pollone ore deposit. In bold, minerals having their type locality at the Pollone mine.

Mineral	Chemical formula	Mineral	Chemical formula
Boulangerite	$Pb_5Sb_4S_{11}$	Owyheeite	$Ag_3Pb_{10}Sb_{11}S_{28}$
Bournonite	$CuPbSbS_3$	**Parasterryite**	$Ag_4Pb_{20}(Sb,As)_{24}S_{58}$
Carducciite	$(AgSb)Pb_6(As,Sb)_8S_{20}$	**Polloneite**	$AgPb_{46}As_{26}Sb_{23}S_{120}$
Chovanite	$Pb_{28}(Sb,As)_{30}S_{72}O$	Proustite	Ag_3AsS_3
Diaphorite	$Ag_3Pb_2Sb_3S_8$	Pyrargyrite	Ag_3SbS_3
Ferdowsiite	$Ag_8Sb_5As_3S_{16}$	Seligmannite	$CuPbAsS_3$
Fettelite	$[Ag_6As_2S_7][Ag_{10}HgAs_2S_8]$	Sterryite	$Cu(Ag,Cu)_3Pb_{19}(Sb,As)_{22}(As–As)S_{56}$
Geocronite	$Pb_{14}Sb_6S_{23}$	Tennantite	$Cu_6Cu_4(Fe,Zn)_2As_4S_{13}$
Jordanite	$Pb_{14}As_6S_{23}$	Tetrahedrite	$Cu_6Cu_4(Fe,Zn)_2Sb_4S_{13}$
Marcobaldiite	$Pb_{12}(Sb_3As_2Bi)_{\Sigma 6}S_{23}$	Twinnite	$PbSbAsS_4$
Meerschautite	$(Ag,Cu)_{5.5}Pb_{42.4}(Sb,As)_{45.1}S_{112}O_{0.8}$	Xanthoconite	Ag_3AsS_3
Meneghinite	$CuPb_{13}Sb_7S_{24}$	Zinkenite	$Pb_9Sb_{22}S_{42}$

mineral was found having the two short unit-cell parameters close to those of jordanite homologues and the longer one intermediate between those of the $N = 3$ and $N = 4$ members, *i.e.* ≈29 Å. The crystallographic and chemical studies allowed its identification as a new homologue belonging to the jordanite series, *i.e.* marcobaldiite, with $N = 3.5$ homologue number. The new mineral and its name have been approved by the CNMNC-IMA (2015-109). The holotype material is deposited in the mineralogical collections of the Museo di Storia Naturale, Università di Pisa, Via Roma 79, Calci, Pisa, Italy, under catalogue number 19709. The name is in honour of the mineral collector Marco Baldi (b. 1944), for his contribution to the knowledge of the mineralogy of the pyrite ± baryte ± iron oxide ore deposits from southern Apuan Alps. Marco Baldi was the first to describe the actual occurrence of geocronite crystals from Valdicastello Carducci (Baldi, 1982). In this way, he contributed to the mineralogical rediscovery of the Pollone mine, which since then has been explored by mineral collectors and mineralogists, leading to the discovery of several rare and new mineral species, mainly represented by lead sulfosalts (sterryite, parasterryite, carducciite, meerschautite, and polloneite – Moëlo *et al.*, 2011; Biagioni *et al.*, 2014; Biagioni *et al.*, 2016b; Topa *et al.*, 2017).

The aim of this paper is the full description of the new mineral species marcobaldiite and the discussion of its crystal-chemistry in the framework of the jordanite homologous series.

2. Geological setting

The baryte + pyrite ± (Pb-Zn-Ag) Pollone ore deposit (latitude 43°57′47″N, longitude 10°16′19″E) is located near Valdicastello Carducci, Pietrasanta, Tuscany, Italy. The ore bodies are hosted within a Paleozoic metavolcanic-metasedimentary sequence, metamorphosed up to greenschist facies conditions during the Alpine orogeny. Estimates of *P*–*T* conditions indicate metamorphic temperatures up to 350 °C with a pressure of 0.35 GPa. Higher *T* values (450 °C) were recorded for mineralizing fluids (Costagliola *et al.*, 1998). Biagioni *et al.* (2016a) described the main geological and structural features of the Pollone mine and distinguished three kinds of occurrence: (i) lenses of microcrystalline baryte + pyrite, with the local presence of interlayers/lenses of galena + sphalerite, folded and partially re-worked during the late tectonic stage evolution of Apuan Alps metamorphic complex (*e.g.*, Carmignani & Kligfield, 1990); (ii) quartz lensoid veins, oriented SW-NE, with coarse-grained masses of galena, sphalerite, and sulfosalts; and (iii) extension quartz ± baryte ± sulfides veins, trending N140–170, embedded both in the country rocks and in the ore bodies.

Twenty-four different sulfosalts have been identified in the Pollone ore deposit (Table 1). The typical occurrence is represented by the microcrystalline baryte + pyrite ore bodies, where sulfosalts are scattered as interstitial grains or as euhedral prismatic to acicular individuals. Rarely, they are related to small quartz + baryte veinlets and small fissures occurring in these ore bodies. This kind of occurrence is typical for the lead-silver sulfosalts from the Pollone mine. The quartz ± baryte ± sulfides extension veins represent another source of sulfosalts. Actually, the well-crystallized specimens of jordanite and geocronite were found in the vugs of these veins. Finally, some Ag sulfosalts have been identified in the quartz lensoid veins oriented SW-NE (*i.e.*, diaphorite and pyrargyrite – Frizzo & Simone, 1995).

3. Occurrence and mineral description

Marcobaldiite was identified in only one sample collected in quartz extension veins embedded in tourmaline-rich schist from the Stanzone tunnel, one of the stopes of the Pollone mine; in the same vein Sb-rich tennantite was identified. Its crystallization is related to the circulation of hydrothermal fluids during the Tertiary Alpine tectono-metamorphic events, favoring the remobilization of elements from the country rocks and the ore bodies and their crystallization in the extension veins (Biagioni *et al.*, 2016a).

Marcobaldiite occurs as a black prismatic crystal measuring 10 mm × 3 mm × 3 mm. The presence of striations suggests the occurrence of a polysynthetic

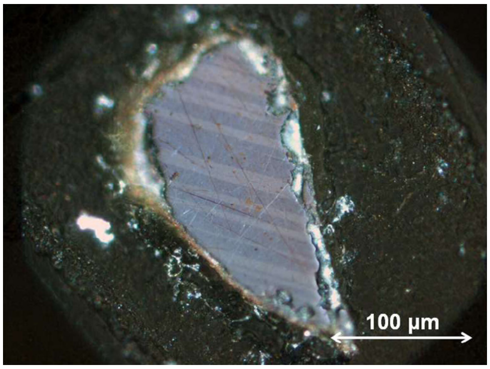

Fig. 1. Reflected light microscopy image of marcobaldiite, showing polysynthetic twinning. Holotype material, Natural History Museum of Pisa University, catalogue number # 19709.

Table 2. Reflectance data (%) for marcobaldiite in air (COM standard wavelengths are given in bold).

λ/nm	R_{min}	R_{max}	λ/nm	R_{min}	R_{max}
400	31.2	35.2	560	30.6	39.0
420	32.3	39.7	580	30.4	38.5
440	32.7	41.7	**589**	**30.4**	**38.5**
460	31.8	40.2	600	30.1	38.4
470	**31.6**	**40.1**	620	30.1	38.1
480	31.8	40.1	640	30.2	38.0
500	31.4	39.9	**650**	**30.0**	**37.6**
520	31.1	39.5	660	29.9	37.6
540	31.0	39.5	680	29.6	36.9
546	**30.9**	**39.6**	700	29.1	36.4

twinning, confirmed by reflected light microscopy (see below). It is brittle, with an irregular fracture. The streak is black, the luster is metallic. Micro-indentation measurements carried out with a VHN load of 15 g give a mean value of 182 kg · mm^{-2} (range: 170–195 kg · mm^{-2}), corresponding to a Mohs hardness of ~3–3½. Density was not measured; calculated density is 6.56 g · cm^{-3}, on the basis of the empirical formula.

In plane-polarized incident light, marcobaldiite is white in color, distinctly bireflectant. Between crossed polars, it is anisotropic, with grey to bluish-grey rotation tints. Internal reflections were not observed. Polysynthetic twinning is common and characteristic (Fig. 1). The reflectance values of marcobaldiite were determined in air with WTiC as standard (Table 2).

3.1. Chemical analysis

A grain of marcobaldiite was analyzed with a Superprobe JEOL JXA 8200 electron microprobe (Eugen F. Stumpfl laboratory, Leoben University, Austria). The operating conditions (WDS mode) were: accelerating voltage 20 kV, beam current 10 nA, beam size 1 µm. Standards (element,

Table 3. Electron microprobe analysis of marcobaldiite: chemical composition as wt% (10 spot analyses) and number of atoms per formula unit (apfu) on the basis of $\Sigma Me = 18$ apfu.

Element	wt%	Range	e.s.d.
Pb	64.05	63.52–64.46	0.34
Bi	4.24	4.16–4.35	0.06
Sb	9.10	8.89–9.38	0.14
As	4.51	4.35–4.62	0.08
S	17.24	16.89–17.42	0.19
Total	99.14	98.29–100.02	0.53
apfu ($Me = 18$)			
Pb	11.98	11.91–12.06	0.04
Bi	0.79	0.77–0.80	0.01
Sb	2.90	2.84–2.96	0.03
As	2.33	2.27–2.40	0.03
S	20.80	20.47–21.11	0.20
Ev (%)	0.8	−0.5–2.6	1.1

Ev (%) = [Σ(val+) − Σ(val−)] × 100/Σ(val−).

emission line) were: galena (Pb *M*α), stibnite (Sb *L*α), GaAs (As *L*α), pyrite (S *K*α), and Bi_2Te_3 (Bi *M*α). Counting times were 30 s on the peak and 15 s on the right and left backgrounds. The studied grain proved to be very homogeneous. Chemical data are given in Table 3.

On the basis of $\Sigma Me = 18$ atoms per formula unit (*apfu*), the empirical formula of marcobaldiite is $Pb_{11.98}Sb_{2.90}As_{2.33}Bi_{0.79}S_{20.80}$. The idealized stoichiometric chemical formula of the studied sample is $Pb_{12}(Sb_3As_2Bi)_{\Sigma 6}S_{21}$, corresponding to (in wt%) Pb 64.02, Sb 9.40, As 3.86, Bi 5.38, S17.34, sum 100.00.

3.2. Crystallography

X-ray powder diffraction pattern of marcobaldiite was collected using a 114.6 mm Gandolfi camera with Ni-filtered Cu *K*α radiation. The observed pattern, compared with the calculated one (obtained using the software PowderCell; Kraus & Nolze, 1996), is reported in Table 4. Owing to the multiplicity of indices for the majority of the observed diffraction lines, the unit-cell parameters were not refined from X-ray powder diffraction data.

Single-crystal X-ray intensity data collection was performed using a Bruker Smart Breeze diffractometer (50 kV, 30 mA) equipped with a CCD 4k low noise area detector. Graphite monochromatized Mo *K*α radiation was used. The detector-to-crystal working distance was 50 mm. A total of 6008 frames was collected in ω scan modes, in 0.25° slices. Exposure time was 25 s per frame. The data were integrated and corrected for Lorentz-polarization, background effects, and absorption, using the package of software *Apex*2 (Bruker, A.X.S. Inc., 2004), resulting in a set of 6790 independent reflections. The refined unit-cell parameters are $a = 8.9248(9)$, $b = 29.414(3)$, $c = 8.5301(8)$ Å, $\alpha = 98.336(5)$, $\beta = 118.175(5)$, $\gamma = 90.856(5)°$, $V = 1944.1(3)$ Å^3. The statistical tests on $|E|$ values ($|E^2 - 1| = 0.993$) suggested the possible

Table 4. X-ray powder diffraction data for marcobaldiite.

I_{obs}	d_{obs}	I_{calc}	d_{calc}	*h k l*	I_{obs}	d_{obs}	I_{calc}	d_{calc}	*h k l*
w	4.45	8	4.406	$\bar{2}$ 1 1	vw	2.553	8	2.568	$\bar{1}$ 10 2
w	3.835	25	3.832	2 1 0	w	2.489	5	2.496	$\bar{2}$ 8 2
w	3.737	6	3.756	$\bar{2}$ 3 0	vw	2.442	3	2.434	$\bar{2}$ 10 1
		5	3.735	$\bar{2}$ $\bar{1}$ 2	mw	2.388	2	2.391	0 8 2
		45	3.692	2 2 0			2	2.385	$\bar{2}$ 10 2
		18	3.683	$\bar{2}$ $\bar{2}$ 2	vw	2.347	1	2.342	1 $\bar{9}$ 2
		20	3.676	0 $\bar{3}$ 2	w	2.294	1	2.297	1 6 2
ms	**3.568**	7	3.596	0 1 2	**vs**	**2.233**	5	2.241	$\bar{1}$ 10 2
		21	3.591	2 $\bar{4}$ 0			48	2.240	2 $\bar{2}$ 2
		25	3.577	$\bar{2}$ $\bar{3}$ 2			6	2.240	$\bar{2}$ 11 2
		40	3.555	0 $\bar{4}$ 2			6	2.229	2 10 0
		17	3.448	0 2 2			5	2.204	0 12 2
m	3.404	17	3.431	$\bar{2}$ $\bar{4}$ 2			46	2.203	$\bar{4}$ 2 2
		26	3.398	2 $\bar{5}$ 0	**s**	**2.125**	7	2.118	3 7 0
		11	3.398	0 $\bar{5}$ 2			54	2.110	$\bar{2}$ 0 4
		14	3.384	$\bar{2}$ 3 2			9	2.107	$\bar{2}$ 12 2
		28	3.314	2 4 0			12	2.094	2 11 0
m	3.256	19	3.274	0 3 2	vw	2.072	13	2.074	0 13 2
		52	3.259	$\bar{2}$ $\bar{5}$ 2	w	2.035	3	2.028	3 8 0
ms	**3.202**	100	3.219	0 9 0	w	2.020	5	2.022	2 13 0
		27	3.219	0 $\bar{6}$ 2	mw	1.980	6	1.986	$\bar{2}$ 13 2
		30	3.208	$\bar{2}$ $\bar{1}$ 2	mw	1.950	20	1.957	$\bar{4}$ $\bar{7}$ 2
m	3.075	29	3.109	2 5 0			6	1.956	0 14 2
		9	3.088	0 4 2	mw	1.911	8	1.916	4 2 0
		30	3.075	$\bar{2}$ $\bar{6}$ 2			6	1.906	2 14 0
ms	**3.016**	28	3.032	0 $\bar{7}$ 2	m	1.878	20	1.895	$\bar{2}$ $\bar{9}$ 4
		12	3.023	$\bar{2}$ 5 2			6	1.880	0 12 2
		35	2.991	2 $\bar{7}$ 0			6	1.868	$\bar{4}$ $\bar{2}$ 4
ms	**2.885**	13	2.908	2 6 0	**s**	**1.848**	9	1.847	$\bar{2}$ 13 2
		36	2.902	0 5 2			17	1.843	2 11 2
m	2.832	10	2.846	0 $\bar{8}$ 2			7	1.839	4 $\bar{7}$ 0
		5	2.841	$\bar{3}$ $\bar{2}$ 2			16	1.835	2 7 2
		20	2.839	$\bar{2}$ 6 2			7	1.811	0 $\bar{7}$ 4
w	2.789	28	2.795	2 $\bar{8}$ 0	vw	1.797	6	1.798	0 2 4
vw	2.756	4	2.755	1 $\bar{5}$ 2	**s**	**1.775**	5	1.778	0 $\bar{8}$ 4
mw	2.707	22	2.721	0 6 2	w	1.753	5	1.749	$\bar{2}$ 14 2
		5	2.720	1 2 2	w	1.716	12	1.705	$\bar{4}$ 11 2
vw	2.652	19	2.662	$\bar{2}$ 7 2	w	1.661	12	1.658	$\bar{2}$ 9 2
w	2.606	6	2.612	2 $\bar{9}$ 0	w	1.608	12	1.609	0 18 0

Note: Intensities and d_{hkl} (in Å) were calculated using the software *PowderCell* 2.3 (Kraus & Nolze, 1996) on the basis of the structural model given in Table 5. The eight strongest reflections are given in bold. Only reflections with $I_{calc} \geq 5$ were reported, if not observed. Observed intensities were visually estimated (vs = very strong; s = strong; ms = medium-strong; m = medium; mw = medium-weak; w = weak; vw = very weak).

centrosymmetricity of marcobaldiite. Consequently, the crystal structure was solved in the space group $P\bar{1}$ using *Shelxs*-97 (Sheldrick, 2008). Scattering curves for neutral atoms were taken from the *International Tables for Crystallography* (Wilson, 1992).

In the first step, the positions of the heavier atoms (Pb, Bi, Sb) were found; through successive difference-Fourier maps, the other atom positions were located. In the crystal structure of marcobaldiite, there are eighteen independent cation positions (one of them split) and twenty-one S sites. Among cation sites, twelve Pb positions and six (Sb/As) sites were identified on the basis of site scattering and *Me*–S distances. The site occupancy factors (s.o.f.) of the Pb positions were initially refined using the scattering curve of Pb *vs* □ and they were found to be fully occupied. The six (Sb/As) positions were refined using the scattering curves of Sb *vs* As. Whereas four of them are mixed (Sb/As) positions, with variable As and Sb contents, Sb4 was found to be completely occupied by Sb only, whereas an atom heavier than Sb partially occupies the site finally labeled Pb9. Consequently, the s.o.f. of this site was modeled using the curve of Pb and Sb, giving a s.o.f. $Pb_{0.61}Sb_{0.39}$. After several cycles of isotropic refinement using *Shelxl*-2014 (Sheldrick, 2015), the R_1 converged to 0.087. By refining the anisotropic displacement parameters for cations only, the refinement yielded a R_1 value of 0.071.

Chemical analysis showed the presence of 0.79 Bi *apfu*. Owing to the similar scattering factors of Pb ($Z = 82$) and Bi ($Z = 83$), it is not possible to distinguish these two atoms on the basis of the site scattering. In order to solve this

Table 5. Crystal data and summary of parameters describing data collection and refinement for marcobaldiite.

Crystal data	
Crystal size (mm)	0.09 × 0.08 × 0.04
Cell setting, space group	Triclinic, $P\overline{1}$
a (Å)	8.9248(9)
b (Å)	29.414(3)
c (Å)	8.5301(8)
α (°)	98.336(5)
β (°)	118.175(5)
γ (°)	90.856(5)
V (Å^3)	1944.1(3)
Z	2
Data collection and refinement	
Radiation, wavelength (Å)	Mo $K\alpha$, $\lambda = 0.71073$
Temperature (K)	293
$2\theta_{max}$ (°)	50.29
Measured reflections	41210
Unique reflections	6790
Reflections with $F_o > 4\sigma(F_o)$	6188
R_{int}	0.0409
$R\sigma$	0.0269
Range of h, k, l	$-10 \leq h \leq 10$, $-34 \leq k \leq 34$, $-10 \leq l \leq 10$
R [$F_o > 4\sigma(F_o)$]	0.0668
R (all data)	0.0702
wR (onF_o^2)	0.2228
Goof	1.093
Number of least-squares parameters	363
Maximum and minimum residual peak (e Å^{-3})	10.88 (at 0.97 Å from Pb14) −3.76 (at 1.05 Å from S8)

indetermination, their bond valence sums (BVS), calculated using the bond parameters of Brese & O'Keeffe (1991), were taken into account. An examination of the BVS at the different Pb and (Pb/Sb) sites suggests that Bi is not preferentially partitioned at any specific position, but it would be statistically distributed among some Pb positions. Bismuth was located in the four Pb sites having the highest BVS values, *i.e.* Pb1, Pb8, Pb15, and Pb16, with a Bi content not exceeding 0.15 *apfu* in each position. The BVS at the Pb9 position, containing 0.39 Sb, agrees with a mixed (Pb,Sb) occupancy, and not with a mixed (Bi, Sb) or (Pb,Sb,Bi) occupancy.

The final anisotropic model for all the atom positions gave $R_1 = 0.067$ for 6188 reflections with $F_o > 4\sigma(F_o)$ and 363 refined parameters. Further details of data collection and refinement are given in Table 5. The occurrence of relatively high maximum and minimum residuals in the difference-Fourier map (*ca.* 11 e Å^{-3}), as well as some short As–S distances at the As17 split position, is a common feature for jordanite homologues (*e.g.*, Biagioni *et al.*, 2016a). It could be likely related to the widespread twinning shown by these minerals and to the possible presence of stacking faults in the alternation of $N = 3$ and $N = 4$ slabs, giving rise to kirkiite-like and jordanite/geocronite domains within marcobaldiite, contributing in this way to the observed disorder.

Atomic coordinates, site occupancy factors, and equivalent isotropic displacement parameters of marcobaldiite are given in Table 6. The unit cell is represented in Fig. 2.

4. Crystal structure description

4.1. General organization

Marcobaldiite is the $N = 3.5$ member of the jordanite homologous series. Following the modular description given by Makovicky *et al.* (2006) for the $N = 3$ homologue kirkiite, the crystal structure of marcobaldiite (Fig. 3) can be described as formed by a stacking sequence of distorted layers of octahedra and trigonal prismatic layers parallel to {0 1 0} and sharing S atoms along their boundaries. $N = 3$ kirkiite-type layers and $N = 4$ jordanite-type layers, three- and four-octahedra thick respectively, alternate along [0 1 0] in a 1:1 ratio, separated by one atomic slab of three bicapped trigonal prismatic (Pb, Bi) atoms and one triangular pyramidal As atom (split position).

Alternatively, the crystal structure can be described as formed by (1 1 1) slabs of distorted PbS archetype (*e.g.*, Moëlo *et al.*, 1985; Makovicky, 1989), or (210) slabs of SnS archetype. The broadness of the two kinds of octahedral layer corresponds to three and four subcells of SnS or PbS. Within each layer, lone-electron-pairs of trivalent Sb and As, at the opposite side of shortest (*i.e.* strongest) (Sb/As)–S bonds, are directed towards a common oblique interspace, to form so-called lone-electron-pair micelles (Fig. 3).

4.2. Cation coordinations and site occupancies

Among cation positions, there are twelve Pb or mixed (Pb, Bi) sites, one pure Sb position, a mixed (Pb, Sb) site, one pure split As position, and three mixed (Sb/As) sites with different As/(As+Sb) atomic ratios. Cation characteristics (selected bond distances, mean bond distances, and bond valence sums) are summarized in Table 7, while bond valence sums on S atoms are given in Table 8.

Lead atoms are six- to eight-fold coordinated, with average bond distances ranging from 2.996 Å for the six-fold coordinated Pb10 site to 3.076 Å for the eight-fold coordinated Pb16 position. Pb3, Pb6, Pb10, and Pb11 have a distorted octahedral coordination; actually, the coordination number of Pb6 is increased to seven when S21b site is occupied. These Pb sites have a pure Pb occupancy, in agreement with their BVS ranging from 1.95 to 1.98 valence unit (*v.u.*). Pb18 have a six-fold coordination corresponding to a trigonal prismatic polyhedron; two additional very long Pb–S bonds, ranging between 3.83 and 3.91 Å, give rise to a bicapped trigonal prism. The Pb atom hosted at this position is underbonded, with a BVS of 1.77 *v.u.* A seven-fold coordination is shown by Pb1, Pb2, Pb7, Pb8, and Pb14 (when S21a is occupied). The occupancies of these sites are represented by Pb only (Pb2, Pb7, and Pb14 sites) or by Pb and Bi atoms (Pb1 and Pb8), with a 85:15 Pb-to-Bi atomic ratio. These agree with the

Table 6. Atomic coordinates, site occupancy factors (s.o.f.), and equivalent isotropic displacement parameters (Å^2) for marcobaldiite.

Site	s.o.f.	*x*	*y*	*z*	U_{eq}
Pb1	$Pb_{0.85}Bi_{0.15}$	0.8503(1)	0.38701(4)	0.4904(2)	0.0199(3)
Pb2	$Pb_{1.00}$	0.8518(1)	0.38638(4)	0.9939(2)	0.0199(3)
Pb3	$Pb_{1.00}$	0.2253(1)	0.49413(4)	0.7368(2)	0.0213(3)
Sb4	$Sb_{1.00}$	0.2412(2)	0.50143(6)	0.2478(2)	0.0116(4)
As5	$As_{0.63(3)}Sb_{0.37(3)}$	0.3689(3)	0.39399(8)	0.0047(3)	0.0171(8)
Pb6	$Pb_{1.00}$	0.3821(2)	0.39554(4)	0.5075(2)	0.0258(3)
Pb7	$Pb_{1.00}$	0.7725(1)	0.16711(4)	0.8456(1)	0.0192(3)
Pb8	$Pb_{0.85}Bi_{0.15}$	0.7695(1)	0.16641(4)	0.3381(2)	0.0194(3)
Pb9	$Pb_{0.61(1)}Sb_{0.39(1)}$	0.0830(2)	0.05688(5)	0.9425(2)	0.0230(3)
Pb10	$Pb_{1.00}$	0.0780(1)	0.05992(4)	0.4471(2)	0.0195(3)
Pb11	$Pb_{1.00}$	0.6128(1)	0.04819(4)	0.9512(2)	0.0201(3)
Sb12	$Sb_{0.98(3)}As_{0.02(3)}$	0.5985(2)	0.05375(6)	0.4500(2)	0.0146(6)
As13	$As_{0.91(3)}Sb_{0.09(3)}$	0.2850(3)	0.15729(9)	0.8444(4)	0.0157(9)
Pb14	$Pb_{1.00}$	0.2937(2)	0.16075(4)	0.3477(2)	0.0243(3)
Pb15	$Pb_{0.85}Bi_{0.15}$	0.4812(2)	0.27712(4)	0.2586(2)	0.0238(3)
Pb16	$Pb_{0.85}Bi_{0.15}$	0.4818(2)	0.27741(4)	0.7431(2)	0.0249(3)
As17a	$As_{0.75(1)}$	0.9939(4)	0.30213(11)	0.2707(4)	0.0146(7)
As17b	$As_{0.25(1)}$	0.9756(12)	0.2494(3)	0.2340(14)	0.0146(7)
Pb18	$Pb_{1.00}$	0.0467(2)	0.27511(4)	0.7796(2)	0.0347(4)
S1	$S_{1.00}$	0.6054(8)	0.3514(2)	0.0996(8)	0.0161(12)
S2	$S_{1.00}$	0.6316(8)	0.3389(2)	0.6100(8)	0.0162(12)
S3	$S_{1.00}$	0.0088(8)	0.4443(2)	0.3618(8)	0.0175(13)
S4	$S_{1.00}$	0.9991(8)	0.4492(2)	0.8435(8)	0.0150(12)
S5	$S_{1.00}$	0.6084(8)	0.4537(2)	0.4324(8)	0.0159(12)
S6	$S_{1.00}$	0.6113(8)	0.4537(2)	0.8754(8)	0.0145(12)
S7	$S_{1.00}$	0.2267(8)	0.3527(2)	0.1134(9)	0.0216(13)
S8	$S_{1.00}$	0.2236(9)	0.3538(2)	0.7092(9)	0.0227(14)
S9	$S_{1.00}$	0.5456(8)	0.1986(2)	0.9932(8)	0.0150(12)
S10	$S_{1.00}$	0.5942(8)	0.2136(2)	0.5278(8)	0.0166(12)
S11	$S_{1.00}$	0.8941(9)	0.1089(2)	0.1302(9)	0.0189(13)
S12	$S_{1.00}$	0.8730(8)	0.1013(2)	0.6092(8)	0.0148(12)
S13	$S_{1.00}$	0.1968(8)	0.0032(2)	0.2106(9)	0.0169(12)
S14	$S_{1.00}$	0.1985(8)	0.0050(2)	0.7444(8)	0.0167(12)
S15	$S_{1.00}$	0.4821(8)	0.0967(2)	0.6306(8)	0.0153(12)
S16	$S_{1.00}$	0.4785(8)	0.0960(2)	0.1916(8)	0.0159(12)
S17	$S_{1.00}$	0.1671(9)	0.1958(2)	0.6078(9)	0.0236(14)
S18	$S_{1.00}$	0.1711(8)	0.1962(2)	0.0017(9)	0.0205(13)
S19	$S_{1.00}$	0.8506(8)	0.2722(2)	0.3915(9)	0.0222(14)
S20	$S_{1.00}$	0.8518(8)	0.2734(2)	0.9742(9)	0.0196(13)
S21a	$S_{0.75(1)}$	0.2244(10)	0.2630(3)	0.3651(10)	0.0111(15)
S21b	$S_{0.25(1)}$	0.233(3)	0.2882(10)	0.381(3)	0.0111(15)

BVS calculation, resulting in values ranging from 1.94 to 2.02 *v.u.* for the pure Pb sites and BVS of 2.11 and 2.07 *v.u.* for the mixed (Pb, Bi) positions. Finally, the Pb15 and Pb16 sites have a bicapped trigonal prismatic coordination and a mixed ($Pb_{0.85}Bi_{0.15}$) site occupancy. Their BVS values are 2.09 and 2.11 *v.u.*, respectively.

Five Me^{3+} positions occur in the crystal structure of marcobaldiite, *i.e.* Sb4, As5, Sb12, As13, and the split site As17. Taking into account the shortest ⟨*Me*–S⟩distances (= the strongest bonds: *Me*–S < 2.70 Å), these sites display a trigonal pyramidal coordination, with *Me* occupying the apex of the pyramid. The coordination sphere is completed by three additional longer bonds. Sb4 is a pure Sb position, with an average ⟨*Me*–S⟩ distance of 2.504 Å and a BVS of 2.94 *v.u.* Antimony is dominant also at the Sb12 position, having a refined s.o.f. of $Sb_{0.98}As_{0.02}$. The average ⟨*Me*–S⟩ distance is 2.462 Å and the BVS indicates moderate overbonding (3.15 *v.u.*). As5, As13, and As17 are three As-dominant positions showing increasing As contents. Indeed, the refined s.o.f. point to $As_{0.63}Sb_{0.37}$, $As_{0.91}Sb_{0.09}$, and $As_{1.00}$, respectively. Actually, the As17 site is split into two sub-positions (As17a and As17b) having a partial occupancy (0.75 and 0.25, respectively) in order to avoid too-short *Me*–*Me* and *Me*–S distances. S21 is also split in two sub-positions S21a and S21b, with s.o.f. 0.75 and 0.25, respectively. As a consequence, As17a, shifted towards the $N = 3$ layer, is bound to S21a, and As17b to S21b.

Taking into account the refined s.o.f. at As5 and As13, the calculated BVS at these positions are relatively high (3.31 and 3.29 *v.u.*, respectively). The higher As contents result in decreasing mean ⟨*Me*–S⟩ distances (2.325 and 2.262 Å for As5 and As13, respectively). The mean bond distances observed at the As17 sub-sites are shorter than

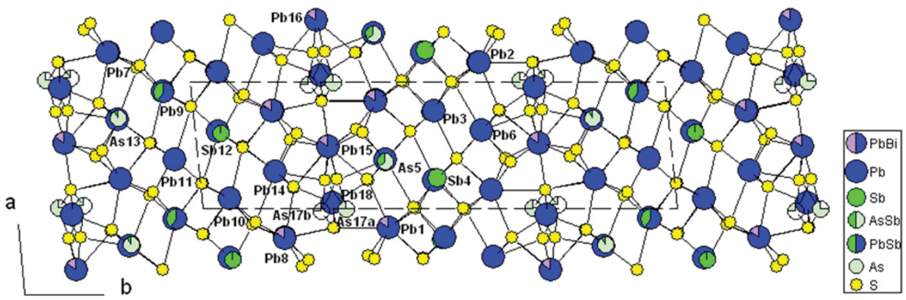

Fig. 2. Projection along **c** of the crystal structure of marcobaldiite.

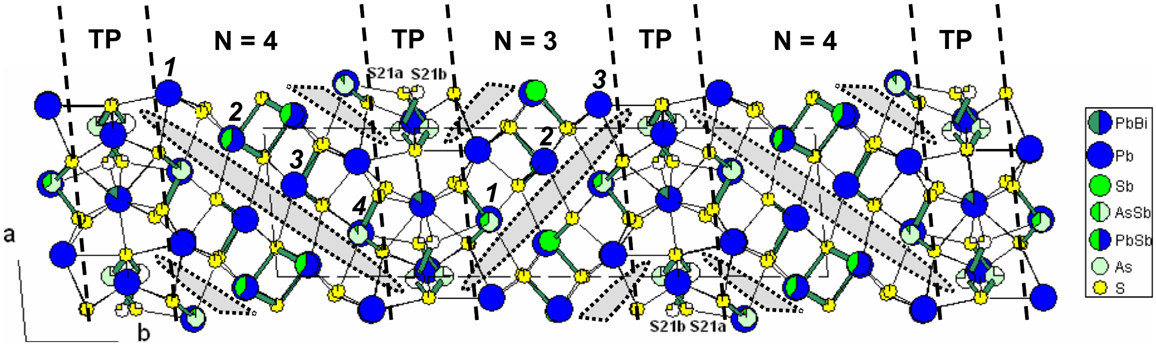

Fig. 3. Modular organization of the crystal structure of marcobaldiite. Alternating oblique $N=3$ and $N=4$ layers are separated by single slabs TP of trigonal prismatic Pb and split As17a/As17b. The three shortest (Sb/As)–S and (Pb,Sb)–S bonds have been enhanced. Shaded ellipses: lone-electron-pair micelles of trivalent Sb and As. Within every N layer, numbers indicate the octahedra sequences.

the ideal one, owing to the average nature of the ligand positions, related to the statistical occupancy of such subsites. This explains the too high BVS obtained (3.35 and 3.74 *v.u.*, assuming the full-occupancy of the sites).

The crystal structure of marcobaldiite is completed by the Pb9 position, within the $N=4$ layer, having a distorted octahedral coordination and an average bond distance of 2.922 Å. The refined s.o.f. points to a mixed site occupancy $Pb_{0.61}Sb_{0.39}$. Assuming such a site occupancy, the corresponding weighted BVS, 2.35 *v.u.*, fits the theoretical one, *i.e.* 2.39 *v.u.*

5. Crystal-chemistry of jordanite homologues

5.1. Structural formula

As described above, the crystal structure of marcobaldiite can be considered as a 1:1 alternation of $N=3$ (kirkiite-type) and $N=4$ (jordanite-type) octahedral layers, separated by a layer formed by Pb trigonal prismatic polyhedra and one As trigonal pyramid (Fig. 3). The $N=3$ layer of marcobaldiite has chemical composition $[Pb_3(Pb_{0.85}Bi_{0.15})(Sb_{1.37}As_{0.63})_{\Sigma 2}S_8]^{-1.85}$. This chemistry can be compared with that given by Makovicky *et al.* (2006) for the $N=3$ octahedral layer in kirkiite, *i.e.* $[Pb_3(Pb_{0.75}Bi_{0.25})(As_{1.42}Bi_{0.58})_{\Sigma 2}S_8]^{-1.75}$. Figure 4 (top) shows the comparison between the $N=3$ layers in marcobaldiite and kirkiite, whereas the site occupancies are compared in Table 9. The $N=4$ layer (Fig. 4, bottom) has chemical composition $[Pb_4(Pb_{0.85}Bi_{0.15})(Pb_{0.61}Sb_{0.39})(Sb_{1.07}As_{0.93})_{\Sigma 2}S_{10}]^{-1.46}$ and can be compared with that of jordanite isotypes from the Pollone mine (Biagioni *et al.*, 2016a), having a chemistry $[Pb_5(Pb_{0.50}Sb_{0.50})(Sb_{0.61\text{-}1.23}As_{1.39\text{-}0.77})_{\Sigma 2}S_{10}]^{-1.5}$. Finally, the layer composed by Pb trigonal prisms and split As site has chemical composition $[Pb(Pb_{0.85}Bi_{0.15})_2AsS_3]^{+3.3}$, to be compared with $[Pb_3AsS_3]^{+3}$ in jordanite isotypes and $[Pb_2(Pb_{0.50}Bi_{0.50})AsS_3]^{+3.5}$ in kirkiite.

The crystal-chemical formula of marcobaldiite can be obtained by the sum of the chemical compositions of the $N=3$, $N=4$ and the trigonal prismatic atomic layers: $[Pb_3(Pb_{0.85}Bi_{0.15})(Sb_{1.37}As_{0.63})_{\Sigma 2}S_8]^{-1.85} + [Pb_4(Pb_{0.85}Bi_{0.15})(Pb_{0.61}Sb_{0.39})(Sb_{1.07}As_{0.93})_{\Sigma 2}S_{10}]^{-1.46} + [Pb(Pb_{0.85}Bi_{0.15})_2AsS_3]^{+3.30} = Pb_8(Pb_{0.85}Bi_{0.15})_4(Pb_{0.61}Sb_{0.39})(As_{2.56}Sb_{2.44})_{\Sigma 5}S_{21}$, that is $Pb_{12.01}(Sb_{2.83}As_{2.44}Bi_{0.60})_{\Sigma 5.99}S_{21}$, to be compared with the formula obtained through chemical analysis, *i.e.* $Pb_{11.98}(Sb_{2.90}As_{2.33}Bi_{0.79})_{\Sigma 6.02}S_{20.80}$. It is close to the ideal stoichiometric formula $Pb_{12}(Sb_3As_2Bi)S_{21}$.

Table 7. Selected bond distances (in Å) and bond-valence sums (BVS − in valence unit, *v.u.*) for cation sites in marcobaldiite.

Pb1	–S3	2.823(6)	Pb2	–S6	2.866(6)	Pb3	–S3	2.692(7)	Pb18	–S19	2.910(7)
	–S5	2.856(6)		–S1	2.963(6)		–S4	2.942(6)		–S20	2.921(7)
	–S4	2.956(6)		–S3	2.989(6)		–S3	2.973(6)		–S17	3.053(7)
	–S1	3.004(6)		–S4	2.999(6)		–S5	3.040(6)		–S8	3.065(7)
	–S2	3.012(6)		–S2	3.009(6)		–S6	3.054(6)		–S18	3.094(7)
	–S8	3.208(7)		–S7	3.224(7)		–S6	3.371(6)		–S7	3.096(7)
	–S19	3.361(7)		–S20	3.303(7)					–S10	3.829(6)
										–S2	3.908(6)
	Average	3.031		Average	3.050		Average	3.012		Average	3.023
	BVS	2.11		BVS	1.94		BVS	1.98		BVS	1.77
Sb4	–S4	2.482(6)	As5	–S7	2.310(7)	Pb6	–S2	2.682(6)			
	–S6	2.496(6)		–S1	2.332(6)		–S5	2.975(6)			
	–S5	2.535(6)		–S8	2.332(7)		–S7	3.022(7)			
	–S4	3.202(6)		–S5	3.411(6)		–S6	3.039(6)			
	–S3	3.217(6)		–S6	3.419(6)		–S8	3.054(7)			
	–S5	3.330(6)		–S4	3.456(6)		–S21b	3.23(3)			
							–S3	3.384(7)			
	Average	2.504		Average	2.325		Average	3.026^1/3.055^2			
	BVS	2.94		BVS	3.31		BVS	1.96			
Pb7	–S15	2.936(6)	Pb8	–S11	2.879(7)	Pb9	–S13	2.679(6)			
	–S9	2.944(6)		–S16	2.936(6)		–S14	2.682(6)			
	–S11	2.962(6)		–S10	2.965(6)		–S13	2.768(7)			
	–S10	2.969(6)		–S9	2.976(6)		–S12	3.069(6)			
	–S12	3.041(6)		–S12	3.031(6)		–S11	3.109(7)			
	–S20	3.112(7)		–S19	3.102(7)		–S16	3.223(6)			
	–S18	3.204(7)		–S17	3.202(7)						
	Average	3.024		Average	3.013		Average	2.922			
	BVS	2.00		BVS	2.07		BVS	2.35			
Pb10	–S14	2.747(6)	Pb11	–S11	2.698(7)	Sb12	–S12	2.450(6)			
	–S12	2.951(6)		–S13	2.960(6)		–S15	2.456(6)			
	–S14	2.978(6)		–S15	3.007(6)		–S16	2.481(6)			
	–S13	3.013(6)		–S14	3.024(6)		–S13	3.320(7)			
	–S11	3.015(6)		–S16	3.025(6)		–S14	3.334(7)			
	–S15	3.270(6)		–S14	3.384(7)		–S13	3.360(7)			
	Average	2.996		Average	3.016		Average	2.462			
	BVS	1.95		BVS	1.95		BVS	3.15			
As13	–S18	2.241(7)	Pb14	–S10	2.694(6)	Pb15	–S21b	2.86(2)			
	–S17	2.270(7)		–S18	2.979(7)		–S21a	2.881(7)			
	–S9	2.276(6)		–S17	3.000(7)		–S2	2.939(6)			
	–S15	3.433(6)		–S21a	3.077(8)		–S19	2.951(6)			
	–S16	3.437(6)		–S16	3.091(6)		–S10	2.983(6)			
	–S12	3.486(7)		–S15	3.128(6)		–S7	3.150(7)			
				–S11	3.355(7)		–S1	3.170(6)			
							–S9	3.248(6)			
							–S18	3.269(7)			
	Average	2.262		Average	3.046^1/3.041^2		Average	3.074^1/3.071^2			
	BVS	3.29		BVS	2.02		BVS	2.09			
Pb16	–S2	2.881(6)	As17a	–S19	2.224(7)	As17b	–S19	2.162(12)			
	–S21b	2.90(3)		–S21a	2.231(8)		–S20	2.190(12)			
	–S21a	2.904(8)		–S20	2.245(7)		–S21b	2.22(3)			
	–S10	2.950(6)		–S7	3.384(7)		–S18	3.445(12)			
	–S20	2.955(6)		–S8	3.394(8)		–S17	3.460(12)			
	–S1	3.170(6)		–S1	3.498(7)		–S9	3.560(12)			
	–S8	3.186(7)									
	–S9	3.252(6)									
	–S17	3.306(7)									
	Average	3.076^1/3.075^2		Average	2.233		Average	2.191			
	BVS	2.11		BVS	2.52		BVS	0.93			

Notes: (i) average bond distances for (Sb/As) sites were calculated taking into account *Me*–S distances shorter than 2.70 Å. (ii) Superscripts "1" and "2" indicate coordinations involving S21a and S21b, respectively. The corresponding BVS involving the split S21 site have been weighted in agreement with the s.o.f. of the sub-positions S21a (0.75) and S21b (0.25). (iii) For sites with mixed occupancy, the BVS have been weighted according to the refined s.o.f. (iv) The average distance at Pb18 site has been calculated taking into account only the six shortest Pb–S distances.

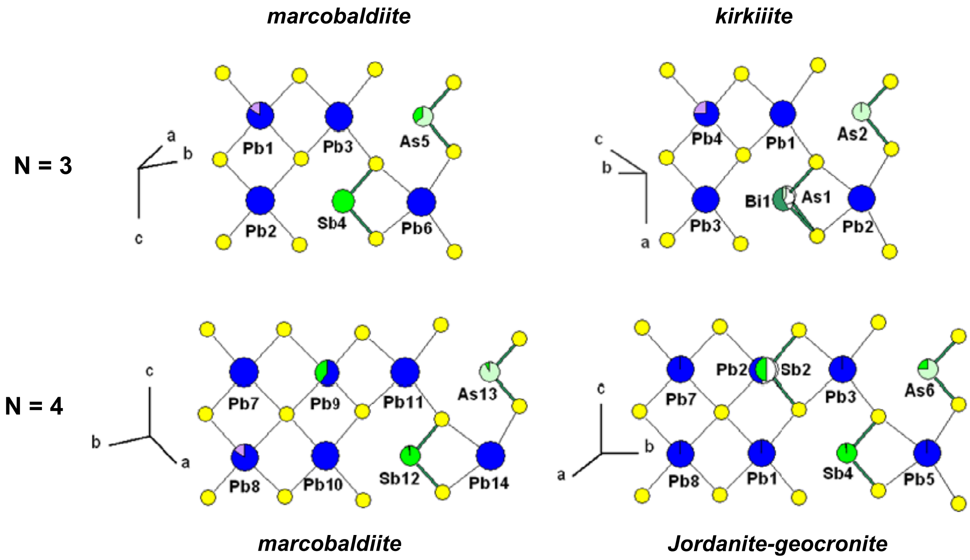

Fig. 4. Comparison between $N = 3$ and $N = 4$ octahedral layers of marcobaldiite with those occurring in kirkiite (top) and jordanite/geocronite (bottom).

Table 8. Bond valence sums (BVS – in valence unit, *v.u.*) for S atoms in marcobaldiite.

Site	BVS	Site	BVS
S1	2.05	S12	2.13
S2	2.06	S13	1.94
S3	2.01	S14	2.01
S4	2.07	S15	2.02
S5	1.96	S16	1.96
S6	1.99	S17	1.90
S7	1.99	S18	1.98
S8	1.92	S19	2.21
S9	1.99	S20	2.13
S10	2.01	S21a	2.12
S11	2.01	S21b	2.09

Note: The BVS at S21a and S21b sites have been calculated assuming their full-occupancy.

All known metalloid ratios of jordanite homologues have been represented in the As-Sb-Bi sub-system (Fig. 5). Taking into account the ideal formulae of geocronite, $Pb_{14}Sb_6S_{23}$, and As-rich kirkiite, $Pb_{10}As_4Bi_2S_{19}$, one can see that the ideal formula of marcobaldiite is quite identical to the 1:1 mixture of these homologues, having formula $Pb_{24}(Sb_6As_4Bi_2)S_{42} = 2 \times Pb_{12}(Sb_3As_2Bi)S_{21}$.

Since Bi is not dominant at any site of the crystal structure of marcobaldiite, the structural formula derived through the single-crystal study could be reduced to a stoichiometric one taking into account the coupled substitution $Pb^{2+} + Sb^{3+} = Bi^{3+} + Pb^{2+}$. Indeed, *ca.* 0.60 Bi *apfu* are distributed among four Pb positions (*i.e.*, Pb1, Pb8, Pb15, and Pb16), whereas Sb is replaced by *ca.* 0.60 Pb *apfu* at the Pb9 position. Subtracting Bi, the structural formula become $Pb_{12}(Sb_{3.44}As_{2.56})_{\Sigma 6}S_{21}$.

5.2. Bismuth in the jordanite homologous series

The occurrence of relatively high contents of Bi in this new mineral species is a rare feature shown by jordanite homologues. Indeed, the findings of high Bi contents in these minerals are limited to three localities, *i.e.* Aghios Philippos, Kirki, Thrace, Greece (Moëlo *et al.*, 1985, 1990); La Fossa crater, Vulcano, Aeolian Islands, Italy (Borodaev *et al.*, 1998; Pinto *et al.*, 2006); and the Pollone mine, Apuan Alps, Tuscany, Italy.

Kirkiite shows Bi contents up to 15.5 and 18.27 wt% in samples from Kirki and Vulcano, respectively (Moëlo *et al.*, 1985; Pinto *et al.*, 2006), corresponding to a maximum content of 3.09 Bi *apfu*, close to the ideal formula $Pb_{10}As_3Bi_3S_{19}$ (Fig. 5). Moreover, Moëlo *et al.* (1990) reported the identification of an Sb-bearing variety of kirkiite, with two samples having average chemical compositions of $Pb_{10.21}(As_{3.48}Sb_{1.36}Bi_{1.16})S_{19.70}$ and $Pb_{10.27}(As_{3.89}Sb_{1.05}Bi_{1.05})S_{19.90}$ (Fig. 5), ideally close to $Pb_{10}(As_4SbBi)S_{19}$. This is the lowest Bi content reported for the $N = 3$ homologue of the jordanite series. The solution of the crystal structure of kirkiite by Makovicky *et al.* (2006) could suggest the cross-substitution of Pb and Bi at the Pb4 and Pb6 positions, with Bi being preferentially partitioned at the Bi1/As1 split site. The chemical variability reported by Moëlo *et al.* (1985, 1990) could be interpreted in the light of this crystal-chemical behaviour, with the composition of the Sb-rich variety corresponding to the occurrence of a mixed $(Bi_{0.50}Sb_{0.50})$ occupancy at the Bi1/As1 site of Makovicky *et al.* (2006). In conclusion, available chemical data suggests that Bi is always present in the $N = 3$ homologue kirkiite.

On the contrary, the $N = 4$ homologues are usually Bi-poor, with Bi contents less up *ca.* 0.50 wt% (*e.g.*, Pollone mine, Apuan Alps, Italy – Biagioni *et al.*, 2016a; Darasun

Table 9. Comparison between site labels and site occupancy factors (s.o.f.) in marcobaldiite, kirkiite, and jordanite/geocronite isotypes.

Marcobaldiite		Kirkiite		Jordanite/geocronite	
Site	s.o.f.	Site	s.o.f.	Site	s.o.f.
Pb1	$Pb_{0.85}Bi_{0.15}$	Pb4	$Pb_{0.75}Bi_{0.25}$		
Pb2	$Pb_{1.00}$	Pb3	$Pb_{1.00}$		
Pb3	$Pb_{1.00}$	Pb1	$Pb_{1.00}$		
Sb4	$Sb_{1.00}$	Bi1/As1	$Bi_{0.58}/As_{0.42}$		
As5	$As_{0.63}Sb_{0.37}$	As2	$As_{1.00}$		
Pb6	$Pb_{1.00}$	Pb2	$Pb_{1.00}$		
Pb7	$Pb_{1.00}$			Pb7	$Pb_{1.00}$
Pb8	$Pb_{0.85}Bi_{0.15}$			Pb8	$Pb_{1.00}$
Pb9	$Pb_{0.61}Sb_{0.39}$			Pb2/Sb2	$Pb_{0.50}/Sb_{0.50}$
Pb10	$Pb_{1.00}$			Pb1	$Pb_{1.00}$
Pb11	$Pb_{1.00}$			Pb3	$Pb_{1.00}$
Sb12	$Sb_{0.98}As_{0.02}$			Sb4	$Sb_{0.61\text{-}0.98}As_{0.39\text{-}0.02}$
As13	$As_{0.91}Sb_{0.09}$			As6	$As_{1.00\text{-}0.75}Sb_{0.00\text{-}0.25}$
Pb14	$Pb_{1.00}$			Pb5	$Pb_{1.00}$
Pb15	$Pb_{0.85}Bi_{0.15}$	Pb7	$Pb_{1.00}$	Pb9	$Pb_{1.00}$
Pb16	$Pb_{0.85}Bi_{0.15}$	Pb6	$Pb_{0.5}Bi_{0.5}$	Pb10	$Pb_{1.00}$
As17	$As_{1.00}$	As3	$As_{1.00}$	As11	$As_{1.00}$
Pb18	$Pb_{1.00}$	Pb5	$Pb_{1.00}$	Pb12	$Pb_{1.00}$

Note: s.o.f. for kirkiite and jordanite/geocronite after Makovicky *et al.* (2006) and Biagioni *et al.* (2016a), respectively.

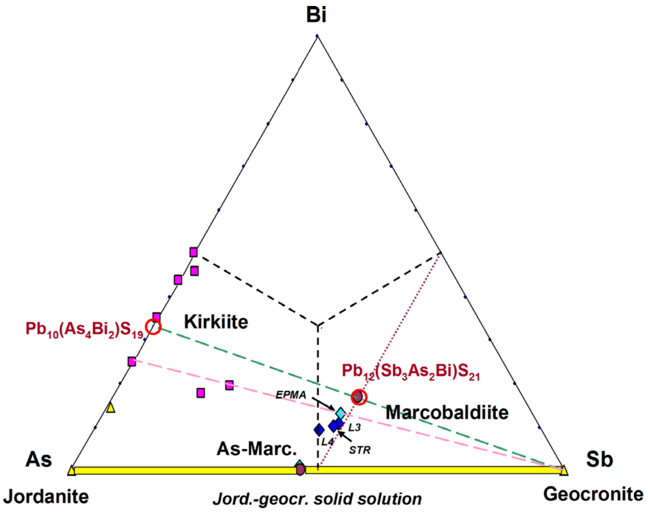

Fig. 5. Projection in the As-Sb-Bi sub-system of various metalloid ratios within the jordanite homologous series. Homologues: $N = 3$, pink squares (kirkiite); $N = 4$, yellow triangles (jordanite and geocronite); $N = 3.5$, lozenges (marcobaldiite and arsenmarcobaldiite). EPMA: microprobe analysis (light blue lozenges); STR: crystal structure (dark blue lozenges), with L3: composition of the kirkiite module (= L3 layer + intermediate slab), and L4: composition of the geocronite module. Brown circles represent ideal compositions of marcobaldiite and arsenmarcobaldiite.

ore deposit, Eastern Transbaikalia, Russia – Bryzgalov *et al.*, 2011). The highest Bi contents were reported by Moëlo *et al.* (1985) on a sample of jordanite associated with type kirkiite, containing up to 4.6 wt% Bi, corresponding to an ideal formula $Pb_{14}As_5BiS_{23}$ (Fig. 5).

According to Fig. 5, the microprobe analysis of marcobaldiite agrees with a mixture of geocronite and (Sb,As)-rich kirkiite. According to its crystal structure, the kirkiite-type component is enriched in Sb relatively to As.

The description of marcobaldiite, characterized by a significant Bi content, similar to that reported for Bi-rich jordanite from Kirki, poses the question about the role of this element in the stabilization of the $N = 3.5$ homologue. As a matter of fact, one could note that Bi-rich jordanite and kirkiite coexist without this intermediate new homologue and could hypothesize that the three pnictogens As, Sb, and Bi are necessary for the crystallization of marcobaldiite. However, Moëlo *et al.* (1990) found Sb-rich kirkiite, showing the simultaneous presence of these three elements; also in this case, no hints about the occurrence of marcobaldiite were found. In addition, the recent finding of the As-rich analogue of marcobaldiite, arsenmarcobaldiite (Biagioni *et al.*, 2016c), substantially devoid of Bi (Bi ≈ 0.30 wt%), seems to discard the hypothesis that this element could play a key role in the formation of the $N = 3.5$ homologue.

5.3. Conditions of formation

The geological history of the baryte + pyrite ore deposit of the Pollone mine is very complex and its origin is still debated (Carmignani *et al.*, 1976; Costagliola *et al.*, 1998). Recently, Biagioni *et al.* (2016a) provided new details for understanding the evolution of the Pollone ore deposit. Indeed, the baryte + pyrite ore bodies have been involved in the Alpine tectono-metamorphic events affecting the rocks belonging to the Apuan Alps metamorphic complex, indicating a pre-Alpine origin of the mineralization. During its late stage evolution, the formation of extension vein systems favored the local remobilization of the ore bodies, giving rise to the peculiar sulfosalt assemblages occurring at the Pollone mine.

The occurrence of Bi is an unusual feature in the framework of the mineralogy of sulfosalts from Apuan Alps, since up to now very few Bi sulfosalts have been identified from the hydrothermal veins (*e.g.*, Orlandi *et al.*, 2010); at the Pollone mine, small amounts of Bi have been reported in sterryite (up to 0.26 wt% – Moëlo *et al.*, 2011) and jordanite/geocronite (up to 0.47 wt% – Biagioni *et al.*, 2016a). According to Moëlo *et al.* (1985), the elemental association of Pb, Bi, and As is typical of thermo-chemical conditions such as high T and weak $f(S_2)$ favoring the incorporation of As as an anion in the crystallizing sulfides (*e.g.*, As-bearing pyrite or arsenopyrite). On the contrary, a high $f(S_2)$ could allow the sulfidation of As and its occurrence in sulfosalts; such a high $f(S_2)$ values could be achieved through the interaction between the hydrothermal solution and a pre-existing sulfide ore deposit. At the Pollone mine, the late recrystallization stage of the baryte + pyrite ore could have locally mobilized As under high $f(S_2)$ conditions, favoring its sulfidation to As^{3+} (Biagioni *et al.*, 2016a), and thus promoting the crystallization of complex Sb-As-(Bi) sulfosalt species. Since it is likely that the stabilization of the $N=3.5$ homologue marcobaldiite is not related to the occurrence of Bi, its crystallization could be related to small local changes in thermo-chemical conditions as well as Pb/(Sb,As,Bi) ratio, sufficient to induce the formation of distinct sulfosalts.

However, the question of the stabilization of marcobaldiite remains open, as this phase has not been observed in experimental studies nor in association with jordanite and kirkiite at Aghios Philippos, Kirki, Greece. Whereas kirkiite and jordanite have been synthesized (*e.g.*, Walia & Chang, 1973), no hints of the $N=3.5$ homologue were found in experimental studies. However, it should be noted that some old chemical analyses of jordanite homologues fit better with the composition $Pb_{12}(Sb/As)_6S_{21}$ than with that of the $N=4$ homologues. As an example, Fisher (1940) reported that the old formula of jordanite was given $Pb_4As_2S_7$, corresponding to one third of the ideal $Pb_{12}As_6S_{21}$ formula of a $N=3.5$ homologue. Likely, such discrepancies were related to inaccuracies in chemical analyses. The composition reported for phase A of Walia & Chang (1973), considered as the synthetic analogue of kirkiite, can be recalculated, on the basis of 6 (As+Bi) *apfu*, as $Pb_{11.57}(As_{4.5\text{-}3.9}Bi_{1.5-2.1})S_{20.57}$, closer to $Pb_{12}(As,Bi)_6S_{21}$ than $Pb_{10}(As,Bi)_6S_{19}$. In this case, the X-ray powder diffraction pattern of phase A seems to agree with that of kirkiite and not with that of marcobaldiite, even if the diffraction patterns of the jordanite homologues are very similar.

Owing to such limitations in old chemical analyses and the similarity in the optical properties as well as in the X-ray powder diffraction patterns with other jordanite homologues, it is likely that the presence of marcobaldiite in sulfosalt assemblages could have been overlooked. The best way to detect marcobaldiite is to perform single-crystal X-ray diffraction studies and systematic and accurate electron-microprobe analyses.

6. Conclusion

The description of marcobaldiite represents a new case of homology in the sulfosalt realm and increases the crystal-chemical complexity of the jordanite homologous series. Makovicky *et al.* (2006) predicted the possible existence of $N=1$, $N=2$, and $N=5$ homologues within the jordanite series. Even if they have not been found yet, the discovery of the $N=3.5$ homologue allows us to hypothesize the existence of other kinds of combination of the $N=3$ and $N=4$ octahedral layers, similarly to what happens in the sartorite homologous series (*e.g.*, Moëlo *et al.*, 2008).

This finding is a further confirmation of the great mineralogical variability of the sulfosalt assemblages from the hydrothermal veins of the Apuan Alps metamorphic complex. The factors controlling the sulfosalt crystallization are not only related to the occurrence of minor components (*e.g.*, Ag, Cu, Hg, Tl), filling specific atom positions, and unique $f(O_2)$ and $f(S_2)$ conditions, promoting the crystallization of oxysulfosalts or persulfosalts; indeed, it seems likely that very subtle variations in the Pb/(Sb,As, Bi) atomic ratios in the crystallizing medium can allow the formation of distinct and original mineral species.

Acknowledgments: On occasion of his 80th birthday, we want to express our gratitude to Stefano Merlino, for his seminal works on mineral crystal-chemistry and modularity. The paper benefited from the constructive comments of Emil Makovicky and an anonymous reviewer. This research received support by MIUR through the SIR 2014 project "THALMIGEN – Thallium: Mineralogy, Geochemistry, and Environmental Hazards", granted to CB (grant no. RBSI14A1CV). The University Centrum for Applied Geosciences (UCAG) is acknowledged for access to the E.F. Stumpfl electron microprobe laboratory.

References

Baldi, M. (1982): La miniera del Pollone a Valdicastello. *Riv. Mineral. Ital.*, **6**, 46–58.

Biagioni, C., Orlandi, P., Moëlo, Y., Bindi, L. (2014): Lead-antimony sulfosalts from Tuscany (Italy). XVI. Carducciite, $(AgSb)Pb_6(As,Sb)_8S_{20}$, a new Sb-rich derivative of rathite from the Pollone mine, Valdicastello Carducci: occurrence and crystal structure. *Mineral. Mag.*, **78**, 1775–1793.

Biagioni, C., Dini, A., Orlandi, P., Moëlo, Y., Pasero, M., Zaccarini, F. (2016a): Lead-antimony sulfosalts from Tuscany (Italy). XX. Members of the jordanite-geocronite series from the Pollone mine, Valdicastello Carducci: occurrence and crystal structures. *Minerals*, **6**, 15.

Biagioni, C., Orlandi, P., Moëlo, Y., Stanley, C.J. (2016b): Lead-antimony sulfosalts from Tuscany (Italy). XVII. Meerschautite, $(Ag, Cu)_{5.5}Pb_{42.4}(Sb, As)_{45.1}S_{112}O_{0.8}$, a new expanded derivative of owyheeite from the Pollone mine, Valdicastello Carducci: occurrence and crystal structure. *Mineral. Mag.*, **80**, 675–690.

Biagioni, C., Merlino, S., Moëlo, Y., Pasero, M., Paar, W.H., Vezzoni, S., Zaccarini, F. (2016c): Arsenmarcobaldiite, IMA 2016-045. CNMNC Newsletter No. 33, October 2016, page 1138. *Mineral. Mag.*, **80**, 1135–1144.

Borodaev, Y.S., Garavelli, A., Kuzmina, O.V., Mozgova, N.N., Organova, N.I., Trubkin, N.V., Vurro, F. (1998): Rare sulfosalts from Vulcano, Aeolian Islands, Italy. I. Se-bearing kirkiite, $Pb_{10}(Bi,As)_6(S,Se)_{19}$. *Can. Mineral.*, **36**, 1105–1114.

Brese, N.E., O'Keeffe, M. (1991): Bond-valence parameters for solids. *Acta Crystallogr.*, **B47**, 192–197.

Bruker, A.X.S. Inc. (2004): APEX 2. Bruker Advanced X-ray Solutions, Madison, Wisconsin, USA.

Bryzgalov, I.A., Krivitskaya, N.N., Spiridonov, E.M. (2011): First find of the minerals of the jordanite-geocronite-schulzite series in one deposit (Darasun, Eastern Transbaikalia). *Doklady Earth Sci.*, **438**, 815–818.

Carmignani, L., Kligfield, R. (1990): Crustal extension in the northern Apennines: the transition from compression to extension in the Alpi Apuane core complex. *Tectonics*, **9**, 1275–1303.

Carmignani, L., Dessau, G., Duchi, G. (1976): Una mineralizzazione sin-tettonica: il giacimento di Valdicastello (Alpi Apuane). Rapporti fra tettonica e minerogenesi in Toscana. *Boll. Soc. Geol. Ital.*, **24**, 725–758.

Costagliola, P., Benvenuti, M., Lattanzi, P., Tanelli, G. (1998): Metamorphogenic barite-pyrite-(Pb-Zn-Ag) veins at Pollone, Apuan Alps, Tuscany: vein geometry, geothermobarometry, fluid inclusions and geochemistry. *Mineral. Petrol.*, **62**, 29–60.

Fisher, D.J. (1940): Discussion of "the formula of jordanite". *Am. Mineral.*, **25**, 297–298.

Frizzo, P., Simone, S. (1995): Diaphorite in the Pollone ore deposit (Apuan Alps, Tuscany, Italy). *Eur. J. Mineral.*, **7**, 705–708.

Jambor, J.L. (1969): New lead sulfantimonides from Madoc, Ontario – Part 3-Syntheses, paragenesis, origin. *Can. Mineral.*, **9**, 505–527.

Kerndt, T. (1845): Über die Krystallform und die chemische Zusammensetzung des Geo-Kronits von Val di Castello. *Ann. Phys.*, **141**, 302–307.

Kraus, W., Nolze, G. (1996): PowderCell – a program for the representation and manipulation of crystal structures and calculation of the resulting X-ray powder patterns. *J. Appl. Crystallogr.*, **29**, 301–303.

Makovicky, E. (1989): Modular classification of sulphosalts – current status. Definition and application of homologous series. *N. Jahr. Miner. Abh.*, **160**, 269–297.

Makovicky, E., Balić-Žunić, T., Karanović, L., Poleti, D. (2006): The crystal structure of kirkiite, $Pb_{10}Bi_3As_3S_{19}$. *Can. Mineral.*, **44**, 178–188.

Matsushita, Y., Momma, K., Miyawaki, R., Sato, A., Kaise, M., Kitazawa, H. (2014): Crystallographic examination of tsugaruite. IMA 2014 Abstract Volume, 331

Moëlo, Y., Oudin, E., Makovicky, E., Karup-Møller, S., Pillard, F., Bornuat, M., Evanghelou, E. (1985): La kirkiite, $Pb_{10}Bi_3As_3S_{19}$, une nouvelle espèce minérale homologue de la jordanite. *Bull. Minéral.*, **108**, 667–677.

Moëlo, Y., Makovicky, E., Karup- Møller, S., Cervelle, B., Maurel, C. (1990): La lévyclaudite, $Pb_8Sn_7Cu_3(Bi,Sb)_3S_{28}$, une nouvelle espèce à structure incommensurable, de la série de la cylindrite. *Eur. J. Mineral.*, **2**, 711–723.

Moëlo, Y., Makovicky, E., Mozgova, N.N., Jambor, J.L., Cook, N., Pring, A., Paar, W.H., Nickel, E.H., Graeser, S., Karup-Møller, S., Balić-Žunić, T., Mumme, W.G., Vurro, F., Topa, D., Bindi, L., Bente, K., Shimizu, M. (2008): Sulfosalt systematics: a review. Report of the sulfosalt sub-committee of the IMA Commission on Ore Mineralogy. *Eur. J. Mineral.*, **20**, 7–46.

Moëlo, Y., Orlandi, P., Guillot-Deudon, C., Biagioni, C., Paar, W., Evain, M. (2011): Lead-antimony sulfosalts from Tuscany (Italy). XI. The new mineral species parasterryite, $Ag_4Pb_{20}(Sb_{14.5}As_{9.5})_{\Sigma 24}S_{58}$, and associated sterryite, $Cu(Ag,Cu)_3Pb_{19}(Sb,As)_{22}(As–As)S_{56}$, from the Pollone mine, Tuscany, Italy. *Can. Mineral.*, **49**, 623–638.

Orlandi, P., Moëlo, Y., Biagioni, C. (2010): Lead-antimony sulfosalts from Tuscany (Italy). X. Dadsonite from the Buca della Vena mine and Bi-rich izoklakeite from the Seravezza marble quarries. *Per. Mineral.*, **79**, 113–121.

Pinto, D., Balić-Žunić, T., Garavelli, A., Garbarino, C., Makovicky, E., Vurro, F. (2006): First occurrence of close-to-ideal kirkiite at Vulcano (Aeolian Islands, Italy): chemical data and single-crystal X-ray study. *Eur. J. Mineral.*, **18**, 393–401.

Sheldrick, G.M. (2008): A short history of SHELX. *Acta Crystallogr.*, **A64**, 112–122.

— (2015): Crystal structure refinement with SHELXL. *Acta Crystallogr.*, **C71**, 3–8.

Shimizu, M., Miyawaki, R., Kato, A., Matsubara, F., Matsuyama, F., Kiyota, K. (1998): Tsugaruite, $Pb_4As_2S_7$, a new mineral species from the Yunosawa mine, Aomori Prefecture, Japan. *Mineral. Mag.*, **62**, 793–799.

Topa, D., Keutsch, F.N., Makovicky, E., Kolitsch, U., Paar, W. (2017): Polloneite, a new complex Pb(-Ag)-As-Sb sulfosalt from the Pollone mine, Apuan Alps, Tuscany, Italy. *Mineral. Mag.*, **81**, 1303–1322.

Walia, D.S., Chang, L.L.Y. (1973): Investigations in the systems $PbS-Sb_2S_3-As_2S_3$ and $PbS-Bi_2S_3-As_2S_3$. *Can. Mineral.*, **12**, 113–119.

Wilson, A.J.C., Ed. (1992): International Tables for X-ray Crystallography, Volume C: Mathematical, physical and chemical tables. Kluwer Academic, Dordrecht, Netherlands.

Received 4 July 2017
Modified version received 13 September 2017
Accepted 15 September 2017